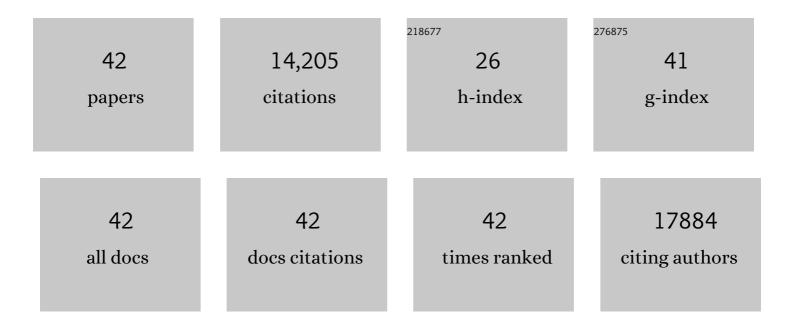
## **Tom Regier**

List of Publications by Year in descending order

Source: https://exaly.com/author-pdf/2405155/publications.pdf Version: 2024-02-01



TOM RECIER

#	Article	IF	CITATIONS
1	Co3O4 nanocrystals on graphene as a synergistic catalyst for oxygen reduction reaction. Nature Materials, 2011, 10, 780-786.	27.5	5,120
2	An Advanced Ni–Fe Layered Double Hydroxide Electrocatalyst for Water Oxidation. Journal of the American Chemical Society, 2013, 135, 8452-8455.	13.7	2,498
3	Homogeneously dispersed multimetal oxygen-evolving catalysts. Science, 2016, 352, 333-337.	12.6	1,948
4	Covalent Hybrid of Spinel Manganese–Cobalt Oxide and Graphene as Advanced Oxygen Reduction Electrocatalysts. Journal of the American Chemical Society, 2012, 134, 3517-3523.	13.7	1,266
5	Catalyst electro-redeposition controls morphology and oxidation state for selective carbon dioxide reduction. Nature Catalysis, 2018, 1, 103-110.	34.4	737
6	Theory-driven design of high-valence metal sites for water oxidation confirmed using in situ soft X-ray absorption. Nature Chemistry, 2018, 10, 149-154.	13.6	476
7	High-valence metals improve oxygen evolution reaction performance by modulating 3d metal oxidation cycle energetics. Nature Catalysis, 2020, 3, 985-992.	34.4	390
8	Golden single-atomic-site platinum electrocatalysts. Nature Materials, 2018, 17, 1033-1039.	27.5	266
9	Nitrogen <i>K</i> -edge XANES – an overview of reference compounds used to identify`unknown' organic nitrogen in environmental samples. Journal of Synchrotron Radiation, 2007, 14, 500-511.	2.4	194
10	Chemical interaction and imaging of single Co3O4/graphene sheets studied by scanning transmission X-ray microscopy and X-ray absorption spectroscopy. Energy and Environmental Science, 2013, 6, 926.	30.8	177
11	Engineering manganese oxide/nanocarbon hybrid materials for oxygen reduction electrocatalysis. Nano Research, 2012, 5, 718-725.	10.4	104
12	Direct Observation of Tetrahedrally Coordinated Fe(III) in Ferrihydrite. Environmental Science & Technology, 2012, 46, 3163-3168.	10.0	84
13	Fe–N bonding in a carbon nanotube–graphene complex for oxygen reduction: an XAS study. Physical Chemistry Chemical Physics, 2014, 16, 15787.	2.8	84
14	Cobalt (II) oxide nanosheets with rich oxygen vacancies as highly efficient bifunctional catalysts for ultra-stable rechargeable Zn-air flow battery. Nano Energy, 2021, 79, 105409.	16.0	74
15	Further Understanding of the Electronic Interactions between N719 Sensitizer and Anatase TiO <sub>2</sub> Films: A Combined X-ray Absorption and X-ray Photoelectron Spectroscopic Study. Journal of Physical Chemistry C, 2011, 115, 5692-5707.	3.1	72
16	Nonstatistical Dopant Distribution of Ln <sup>3+</sup> -Doped NaGdF <sub>4</sub> Nanoparticles. Journal of Physical Chemistry C, 2011, 115, 15950-15958.	3.1	57
17	Observation of the origin of d <sup>0</sup> magnetism in ZnO nanostructures using X-ray-based microscopic and spectroscopic techniques. Nanoscale, 2014, 6, 9166.	5.6	57
18	Manganese-Driven Carbon Oxidation at Oxic–Anoxic Interfaces. Environmental Science & Technology, 2018, 52, 12349-12357.	10.0	54

Tom Regier

#	Article	IF	CITATIONS
19	Spectroscopic understanding of ultra-high rate performance for LiMn0.75Fe0.25PO4 nanorods–graphene hybrid in lithium ion battery. Physical Chemistry Chemical Physics, 2012, 14, 9578.	2.8	48
20	Speciation and distribution of copper in a mining soil using multiple synchrotron-based bulk and microscopic techniques. Environmental Science and Pollution Research, 2014, 21, 2943-2954.	5.3	44
21	Soft X-ray Induced Photoreduction of Organic Cu(II) Compounds Probed by X-ray Absorption Near-Edge (XANES) Spectroscopy. Analytical Chemistry, 2011, 83, 7856-7862.	6.5	38
22	Revealing the charge/discharge mechanism of Na–O <sub>2</sub> cells by <i>in situ</i> soft X-ray absorption spectroscopy. Energy and Environmental Science, 2018, 11, 2073-2077.	30.8	37
23	Transforming reed waste into a highly active metal-free catalyst for oxygen reduction reaction. Nano Energy, 2019, 62, 700-708.	16.0	37
24	The Origin and Dynamics of Soft Xâ€Rayâ€Excited Optical Luminescence of ZnO. ChemPhysChem, 2010, 11, 3625-3631.	2.1	34
25	Temperature resolved alteration of soil organic matter composition during laboratory heating as revealed by C and N XANES spectroscopy and Py-FIMS. Thermochimica Acta, 2012, 537, 36-43.	2.7	30
26	Advances in Using Soft X-Ray Spectroscopy for Measurement of Soil Biogeochemical Processes. Advances in Agronomy, 2015, , 1-32.	5.2	30
27	Aircraft and MiniCAST soot at the nanoscale. Combustion and Flame, 2019, 204, 278-289.	5.2	28
28	Cultivation Affects Soil Organic Nitrogen: Pyrolysisâ€Mass Spectrometry and Nitrogen Kâ€edge XANES Spectroscopy Evidence. Soil Science Society of America Journal, 2009, 73, 82-92.	2.2	27
29	Time-Resolved X-ray Excited Optical Luminescence from Tris(2-phenyl bipyridine)iridium. Journal of the American Chemical Society, 2006, 128, 3906-3907.	13.7	26
30	The unexpected structures of "core–shell―and "alloy―LnF3 nanoparticles as examined by variable energy X-ray photo-electron spectroscopy. Nanoscale, 2011, 3, 3376.	5.6	26
31	TG–FTIR, LC/MS, XANES and Py-FIMS to disclose the thermal decomposition pathways and aromatic N formation during dipeptide pyrolysis in a soil matrix. Journal of Analytical and Applied Pyrolysis, 2011, 90, 164-173.	5.5	23
32	Soil organic matter characteristics as indicator of Chernozem genesis in the Baltic Sea region. Geoderma Regional, 2016, 7, 187-200.	2.1	20
33	Soil organic matter characteristics in drained and rewetted peatlands of northern Germany: Chemical and spectroscopic analyses. Geoderma, 2019, 353, 468-481.	5.1	19
34	The structure of haplobasaltic glasses investigated using X-ray absorption near edge structure (XANES) spectroscopy at the Si, Al, Mg, and O K -edges and Ca, Si, and Al L 2,3 -edges. Chemical Geology, 2016, 420, 213-230.	3.3	18
35	Probing the Structure of NaYF <sub>4</sub> Nanocrystals using Synchrotron-Based Energy-Dependent X-ray Photoelectron Spectroscopy. Journal of Physical Chemistry C, 2014, 118, 21639-21646.	3.1	15
36	X-ray Excited Optical Luminescence from Diamond Thin Films:Â The Contribution of sp2- and H-Bonded Carbon to the Luminescence. Journal of the American Chemical Society, 2007, 129, 1476-1477.	13.7	14

Tom Regier

#	Article	IF	CITATIONS
37	High-energy and high-power Zn–Ni flow batteries with semi-solid electrodes. Sustainable Energy and Fuels, 2020, 4, 4076-4085.	4.9	14
38	Bulk sensitive determination of the Fe <sup>3+</sup> /Fe <sub>Tot</sub> -ratio in minerals by Fe L <sub>2/3</sub> -edge X-ray Raman scattering. Journal of Analytical Atomic Spectrometry, 2016, 31, 815-820.	3.0	9
39	Zinc Porphyrinâ€Ðriven Assembly of Gold Nanofingers. Small, 2008, 4, 497-506.	10.0	8
40	Chemistry and Associations of Carbon in Water-Stable Soil Aggregates from a Long-Term Temperate Agroecosystem and Implications on Soil Carbon Stabilization. ACS Agricultural Science and Technology, 2021, 1, 294-302.	2.3	1
41	Direct Observation of Optical Band Gap Components in Ga1–xZnxN1–xOx Solid-Solution Nanoparticles. Journal of Physical Chemistry C, 2021, 125, 19438-19444.	3.1	1
42	Positronâ€emitting radiotracers spatially resolve unexpected biogeochemical relationships linked with methane oxidation in Arctic soils. Global Change Biology, 2022, , .	9.5	0